Virology **265,** 274–285 (1999)
Article ID viro.1999.0045, available online at http://www.idealibrary.com on IDEAL®

Insertional Mutagenesis of AAV2 Capsid and the Production of Recombinant Virus

Joseph E. Rabinowitz,* Weidong Xiao,† and R. Jude Samulski*,[1]

*The Gene Therapy Center, University of North Carolina at Chapel Hill, Chapel Hill, North Carolina 27599; and †Institute for Human Gene Therapy, University of Pennsylvania, Philadelphia, Pennsylvania 19104

Received August 2, 1999; returned to author for revision August 30, 1999; accepted October 11, 1999

The structural genes of adeno-associated virus serotype 2 (AAV2) have been altered by linker insertional mutagenesis in order to define critical components of virion assembly and infectivity. An in-frame restriction site linker was inserted across the capsid coding domain of a recombinant plasmid. After complementation *in vivo,* recombinant AAV2 viruses were generated and assayed for capsid production, packaging, transduction, heparin agarose binding, and morphology. Three classes of capsid mutants where identified. Class I mutants expressed structural proteins but were defective in virion assembly. Class II mutants generated intact virions that protected the viral genome from DNase, but failed to infect target cells. The majority of these mutants bound the heparin affinity matrix, suggesting that attachment to the AAV primary receptor was not rate limiting. One class II mutant, H2634, assembled virions and bound heparin using only Vp3, indicating that this subunit is responsible for mediating AAV receptor attachment. Finally, class III mutants assembled virions, encapsidated DNA, and infected target cells. Infectivity of these mutants ranged from 5 to 100% of that of the wild-type, demonstrating for the first time the ability to alter capsid proteins without interfering with infectivity. These AAV virions with altered capsid subunits will provide critical templates for manipulating AAV vectors for cell-specific gene delivery *in vivo.* In summary, the AAV capsid variants described here will facilitate further study of virus assembly, entry, and infection, as well as advance the development of this versatile vector system.

INTRODUCTION

Adeno-associated virus serotype 2 (AAV2) is a small nonenveloped virus in the parvoviridae family that requires a helper virus, adenovirus or herpesvirus, for efficient productive infection (Casto *et al.,* 1967; McPherson *et al.,* 1985). AAV2 packages a 4681-nucleotide (Srivastava *et al.,* 1983) genome of both positive and negative polarity (Berns and Adler, 1972; Berns and Rose, 1970; Rose *et al.,* 1969) into a 20- to 25-nm virion with icosahedral symmetry (Atchison *et al.,* 1965; Hoggan *et al.,* 1966). The viral DNA consists of two open reading frames flanked by inverted terminal repeats. The right open reading frame, which is expressed from the p40 promoter, codes for three structural proteins Vp1, Vp2, and Vp3. The regions that encode the three capsid genes share overlapping reading frames. The capsid genes are regulated by alternative splicing (Vp1) and translational initiation (ACG for Vp2 and AUG for Vp3) during a productive infection (Becerra *et al.,* 1988; Muralidhar *et al.,* 1994; Su *et al.,* 1996; Trempe and Carter, 1988). After translation, the capsid proteins migrate to the nucleus and assemble into progeny virions. The virions are composed of 60 subunits with a stoichiometry of 1:1:20 for Vp1, Vp2, and Vp3, respectively (Rose *et al.,* 1971). The ratio of virion capsid subunits correlates with *in vivo* expression levels seen during productive infection.

Early studies of AAV2 support the idea that all three capsid subunits are required to extract single-stranded genomes from the pool of replicating double-stranded DNA. These genomes are then sequestered into preformed immature particles that maturate to infectious particles. These particles have a density between 1.32 and 1.41 g/mL in cesium chloride and sediment between 60 and 125S in sucrose (Myers and Carter, 1981; Myers *et al.,* 1980). Mutagenesis studies of AAV2 capsids have shown that insertions and deletions in the Vp3 domain completely inhibit the accumulation of single-stranded virions and production of infectious particles (Hermonat *et al.,* 1984; Ruffing *et al.,* 1994). Missence mutagenesis of Vp1, Vp2, and Vp3 initiation codons resulted in no accumulation of single-stranded template or production of infectious particles (Muralidhar *et al.,* 1994), suggesting an essential role for the individual capsid subunits during a productive infection. In contrast, it has been shown that a 186-bp *Xho*I deletion in the unique coding region of Vp1 does not inhibit accumulation of single-stranded template, but results in low infectious particles (Hermonat *et al.,* 1984; Janik *et al.,* 1984; Tratschin *et al.,* 1984). The use of an amber mutation, which decreased production of Vp1 to 5% of wild-type levels in an amber suppressor cell line, was still sufficient for the accumulation of single-stranded DNA and production of infec-

[1] To whom reprint requests should be addressed at Gene Therapy Center, University of North Carolina at Chapel Hill, 7119 Thurston-Bowles CB7352, Chapel Hill, NC 27599-7352. Fax: (919) 966-0907. E-mail: rjs@med.unc.edu.

0042-6822/99 $30.00

tious particles (Smuda and Carter, 1991). In fact 45% of the Vp1 unique region can be deleted or >90% of the protein depleted using the amber suppressor mutation and low infectious particles still form (Hermonat *et al.,* 1984; Janik *et al.,* 1984; Smuda and Carter, 1991; Tratschin *et al.,* 1984). These studies suggest that accumulation of single-stranded DNA requires the presence of Vp1 but the levels may be variable and insertions and deletions can be tolerated. While mutant analysis of the Rep coding region has been more extensive than that of the capsid coding region, the above analyses have been informative about the role of structural proteins in AAV assembly.

In fact, now several studies have demonstrated that parvovirus capsid proteins can be mutated and virion assembly studied. In one study, the coding region for 147 amino acids of the hen egg white lysozyme was substituted for the B19 Vp1 unique coding sequence. This modification resulted in purified empty particles that retained lysozyme enzymatic activity (Miyamura *et al.,* 1994). In addition, expression of peptides (9 and 13 residues) in B19 Vp2 resulted in empty particles that were immunogenic in mice supporting surface presentation of the insertions (Brown *et al.,* 1994). In a more recent study, the CD8 + CTL epitope (residues 118–132) against lymphocytic choriomeningitis virus (LCMV) nucleoprotein was inserted into the Vp2 capsid protein of porcine parvovirus (ppv) (Sedlik *et al.,* 1997). This capsid protein with the epitope cloned at the N-terminus self-assembled when expressed in a baculovirus system. This chimeric virus-like particle was then used to immunize mice against a lethal challenge from LCMV (Sedlik *et al.,* 1997). These studies establish the flexibility of the B19 and ppv capsids when foreign sequences are inserted into domains outside the predicted core β-barrel motif when using empty particles.

The identification of domains that are responsible for AAV2 host range, binding to the major cell surface receptor, and domains that can accommodate insertions without loss of function is important for a virus that is being considered as a candidate vector for human gene therapy. Mutagenesis along with a crystal structure should provide sufficient details to characterize the role of the AAV structural subunits in virion assembly and infectivity. However, in the absence of a crystal structure, we have used linker insertion mutagenesis to isolate a collection of mutants throughout the capsid coding region. Using Western blot, electron microscopy (EM) analysis, DNase protection, and virion transduction assays, we have identified three classes of insertion mutants. Class I mutants are defective for virions assembly and/or stability. Class II mutants protect viral DNA from DNase digestion but are not infectious, while class III mutants express foreign peptides and maintain morphology, stability, and infectivity of the wild-type virion. This unique assortment of viable insertion mutants will be critical reagents for studying AAV assembly and infectivity as well as serve as templates for the development of targeting AAV vectors for human gene therapy.

RESULTS

Construction of insertional mutations in rAAV2

In order to evaluate the role of AAV structural proteins in assembly and infectivity, we generated a collection of capsid linker insertion mutants. A 2.8-kb *Hin*dIII fragment of pAAV/Ad (Samulski *et al.,* 1989) containing the sequences coding for the capsid domain of AAV2 was subcloned into pBS^{+}. This plasmid, pAV2Cap, was used for partial digestion with *Hae*III, *Nla*IV, and *Rsa*I to generate a substrate for capsid-specific insertions (Fig. 1). These three DNA restriction enzymes constitute 43 sites that span the AAV-2 capsid coding sequence, of which only 4 overlap. To efficiently identify clones that contain insertions, a kanamycin resistance gene (Kan^{r}) flanked by a novel oligo (*Nae*I/*Eco*RV) was ligated with partially digested, full-length, linearized pAV2Cap (see Materials and Methods for details and Fig. 1). Using ampicillin and kanamycin selection in *Escherichia coli,* insertion mutants were identified and the Kan^{r} gene was shuttled out of the capsid coding region by digesting and religation with the nested pair of *Eco*RV sites (see Materials and Methods). This resulted in a specific linker insertion of 12-bp carrying a single copy of the unique *Eco*RV site in the capsid coding sequences. The exact positions of the linker insertion were further refined by restriction enzyme digestions and, in six cases, sequencing (data not shown). The position of insertion mutants are identified by the first letter of the enzyme used in the partial digestion followed by the nucleotide position of the restriction site in the AAV2 genome, for example, *Nla*IV 4160 would be N4160.

The capsid coding sequence from these mapped insertion mutants were subcloned into the helper vectors pACG2 or pAAV/Ad for biological characterization *in vivo* (Fig. 1) (Li *et al.,* 1997; Samulski *et al.,* 1989). Sequence analysis predicts that this 12-bp insertion cannot result in a termination codon for any of the 43 insertion sites (Table 1). Owing to the random nature of the cut site for the enzymes (*Hae*III, *Nla*IV, and *Rsa*I) with respect to codon frame usage and the degeneracy of the *Nla*IV recognition sequence, the 12-bp linker resulted in the insertion of the amino acids GDIA in frame 1 and AISP in frame 3 for all three enzymes, while insertions in frame 2 resulted in WRYR**H** for *Rsa*I, **G**RYRP for *Hae*III, and both **G**RYRP and GRYR**H** for *Nla*IV. The bold-faced amino acids in these examples represent missense mutations (Table 1). The mutant helper constructs, pACG2^{IN}, were individually transfected into 293 cells along with an AAV reporter vector, containing the β-galactosidase gene in adenovirus *dl*309 (M.O.I. = 5)-infected cells (Li *et al.,* 1997). The transfected cells were then assayed for cap-

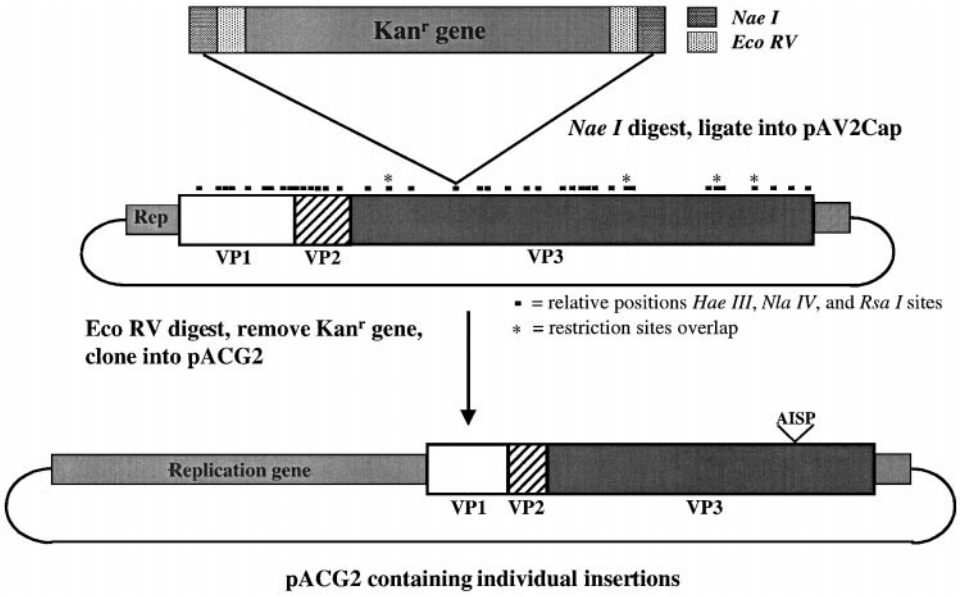

FIG. 1. Insertional mutagenesis strategy for AAV2 capsid. A cassette containing the kan^r gene flanked by *Eco*RV and *Nae*I sites were cloned into the plasmid pAV2Cap. pAV2Cap, which contains the open reading frame of AAV2 capsid, was partially digested with *Hae*III, *Nla*IV, and *Rsa*I separately so that unit-length products were isolated. The 43 positions of restriction sites for these enzymes are shown above the diagram of the capsid open reading frame. The position of the Kan^r insert was mapped by restriction enzyme digestion and in some cases sequenced. Once the position was determined the Kan^r gene was removed by *Eco*RV digestion, and the capsid domain subcloned into pACG. This strategy resulted in inserting a 12-bp fragment, with half the *Nae*I sites flanking a unique *Eco*RV site, into the respective *Hae*III, *Nla*IV, and *Rsa*I sites. The 12 bp code for four amino acids, one of which is shown above the diagram of pACG2.

sid expression and recombinant virus production (see Materials and Methods) (Li *et al.,* 1997).

Analysis of capsid proteins

Before assaying for vector production using mutant capsid constructs in complementation assays, each insertion mutant was tested for expression of capsid subunits in 293 cells after transfection. The ability to produce Vp1, Vp2, and Vp3 at normal stoichiometry would suggest that linker insertions did not alter capsid protein expression or stability. Since the linker did not introduce stop codons, it was expected that each insert would produce all three capsids. Forty-eight hours after transfection, cell lysates were analyzed by Western blot for AAV capsids. The Western blot analysis in Fig. 2 is a representation of insertion mutant capsid expression in cell lysates. With the exception of H2634 (Fig. 2, lane 2), the stoichiometry of the three capsid subunits does not appear significantly different than that of wild-type controls (Fig. 2 compare lanes 1, 3–7 to lane 8). By this assay, insertion mutant H2634 appears to produce only Vp3 subunits (Fig. 2, lane 2). In longer exposures, the minor capsid subunits in Fig. 4, lanes 4 and 5, were apparent (data not shown).

Mutant capsid ability to produce stable virions

To test for the production of stable virions that protect a vector genome from DNase digestion, we subjected the cell lysates to cesium chloride (CsCl) gradient centrifugation. Virus densities were measured by refractometry, and aliquots from appropriate fractions were subjected to dot blot hybridization (Fig. 3A). Based on this analysis, particles that package intact recombinant genomes should display a buoyant density similar to that of the wild-type and be resistant to DNase treatment, with the exception of H2944, which has a buoyant density slightly higher than that of the wild-type. Results for this assay separated insertion mutants into two classes. Class I mutants were negative for protecting the viral genome, while class II mutants appeared normal for packaging and protecting the vector substrate (Table 1).

All class II mutants had a buoyant density within the range of that of wild-type AAV2 capsids (Fig. 3A). By dot blot analysis, N2944 packaged the recombinant genome but migrated to a position of slightly greater density than wild-type in isopycnic gradients (Fig. 3A, N2944, lane 3). A number of insertion mutants (7) did not package DNA by this assay, which had a sensitivity of $<1 \times 10^5$ particles/μl (see Materials and Methods for quantitation) (Table 1). Whether these mutants were defective in packaging or unstable during purification remains to be determined.

Infectivity of class II insertion mutants

Virions generated by insertion mutants in the complementation assay were tested for infectivity by monitoring

TABLE 1

Physical Structure and Phenotype of AAV2 Capsid Insertion Mutants

Position[a] inserted	Capsid subunit	Frame[b]	Dot blot[c]	Infectious[d]	Heparin agarose[e]	Electron microscope	Phenotype	Amino acid[f]
H2285	VP1	3	2.8×10^7	−	+	Normal	Class II	AISP
R2356	VP1	2	1.4×10^8	+	+	N.D.	Class III	WRYR**H**
N2364	VP1	1	—	−	N.D.	N.D.	Class I	GDIA
H2416	VP1	2	1.4×10^7	−	+	N.D.	Class II	**G**RYRP
H2591	VP1	3	1.4×10^7	+	+	Normal	Class III	AISP
H2634	VP2	1	2.8×10^7	−	+	Normal	Class II	GDIA
H2690	VP2	3	7.0×10^6	+	+	Normal	Class III	AISP
R2747	VP2	3	—	−	N.D.	N.D.	Class I	AISP
H/N2944	VP3	2	1.4×10^6	+[g]	N.D.	N.D.	Class II/III	**G**RYRP
N3317	VP3	3	1.4×10^5	−	N.D.	N.D.	Class II	AISP
R3391	VP3	2	—	−	N.D.	N.D.	Class I	WRYR**H**
N3561	VP3	1	—	−	N.D.	N.D.	Class I	GDIA
H3595	VP3	2	1.4×10^6	+[g]	N.D.	Abnormal	Class II/III	**G**RYRP
H/N3761	VP3	3	1.4×10^7	−	−	Normal	Class II	AISP
H3766	VP3	2	2.8×10^7	−	N.D.	N.D.	Class II	**G**RYRP
N4046	VP3	3	—	−	N.D.	N.D.	Class I	AISP
H/N4047	VP3	1	—	−	N.D.	N.D.	Class I	GDIA
N/R4160	VP3	3	1.4×10^7	+	+	Normal	Class III	AISP

[a] The letter refers to the restriction enzyme used in the partial digestion and the number refers to the nucleotide of the restriction site in the AAV2 sequence.

[b] Reading frame of the restriction site.

[c] The particle number per microliter of sample. (−) = $<10^5$ genomes.

[d] Infections were done using 1.75×10^8 particles of rAAV insertion mutants in adenovirus-infected HeLa cells.

[e] By batch binding and assayed by infection of HeLa cells (class III) or by dot blot (class II).

[f] Amino acids differ depending on the frame of the insertion. The amino acid in boldface is a missense mutation.

[g] Infectious only when purified using Iodixanol.

transduction of LacZ reporter gene in human cells. Using viral titers derived from dot blot hybridization, HeLa cells were infected with mutant virus stocks at equivalent particle numbers. Twenty-four hours postinfection, expression of the transgene was detected by X-gal staining. A representative figure of this analysis is shown (Fig. 3B) and all mutants assayed are presented in Table 1. In this assay, wild-type virions transduced 5.6×10^5 HeLa cells/1.75×10^8 protected particles (Fig. 3B and Materials and Methods). Based on the sensitivity of this assay, the range of infection efficiency for class II insertion mutant viruses was from 0 to 1.6×10^6 transducing units/1.75×10^8 protected particles. Results from this analysis further subdivided the capsid insertion mutants from class II (normal for packaging and protecting the vector substrate) into a class III phenotype (normal for packaging and protecting the vector substrate and infectious virions). Two insertion mutants negative for infectivity and initially identified as class II mutants (N2944, H3595) based on CsCl purification and DNase protection tested positive for viral transduction after purification using an iodixanol step gradient (Table 1). This virus

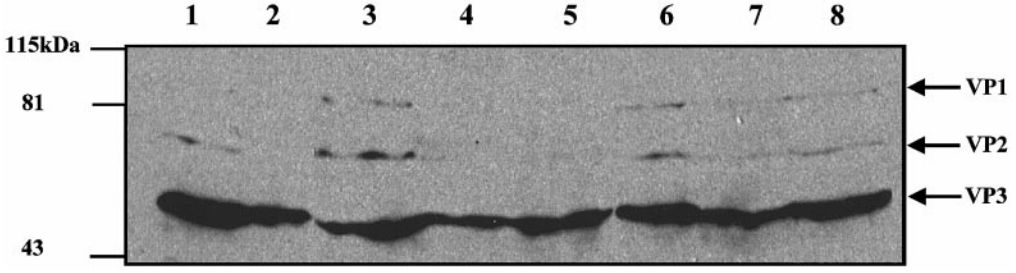

FIG. 2. Expression of capsid proteins in cells transfected with wild-type and insertion mutant helper plasmids of pACG2. Cell lysates from 293 cells transfected with 1, H2285; 2, H2634; 3, H2690; 4, N2944; 5, H2944; 6, H3595; 7, H4047; 8, wild-type were analyzed by acrylamide gel electrophoresis and immunoblotting with the B1 monoclonal antibody and detected by peroxidase-conjugated secondary antibody. On the left of the Western blot are the positions of the molecular weight standards and on the right are the positions of the major capsid protein, VP3, and the minor capsid proteins, VP2 and VP1.

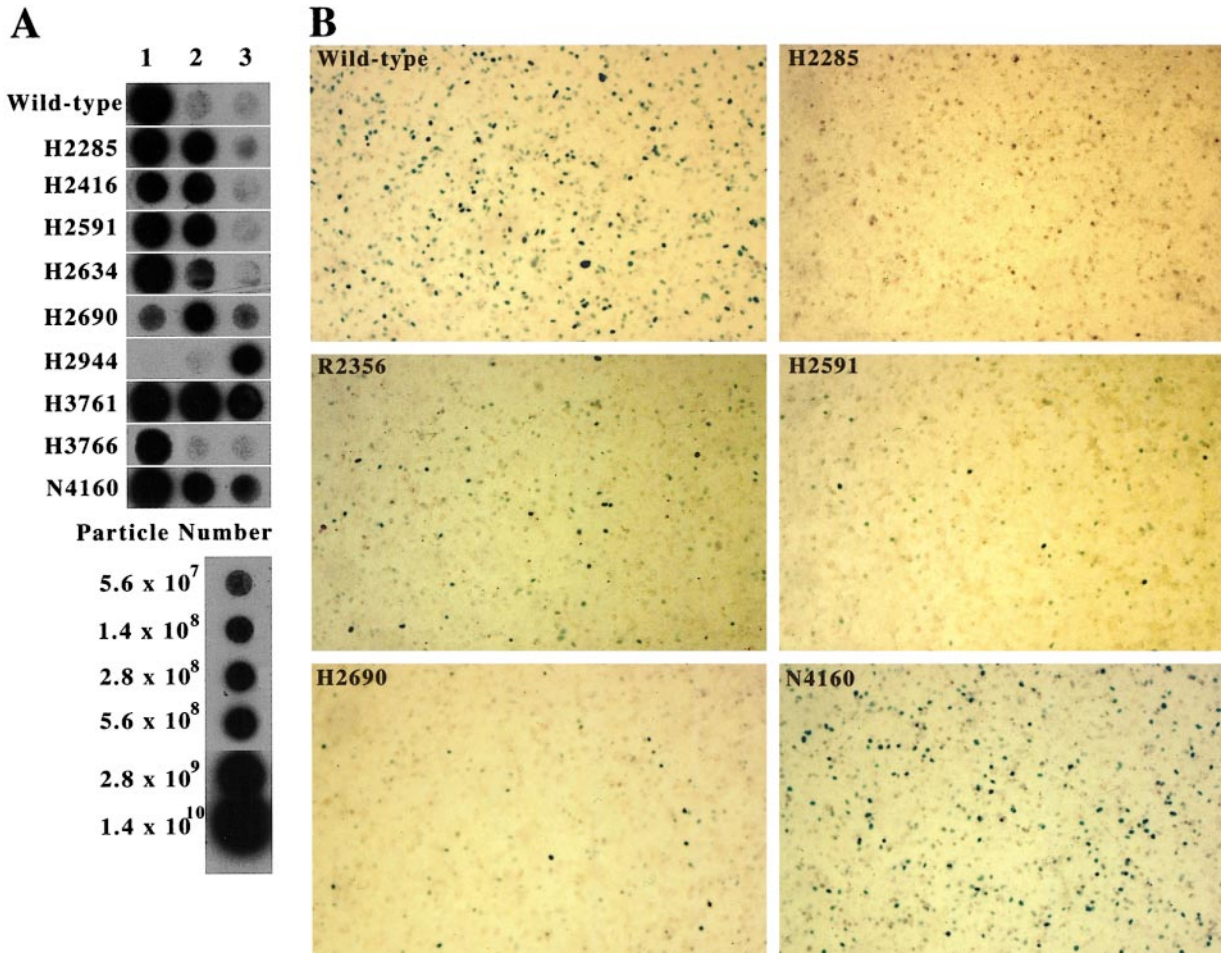

FIG. 3. (A) Dot blot hybridization to the LacZ transgene. Cell lysates of adenovirus-infected 293 cells transfected with the insertion mutant or wild-type helper plasmids and the LacZ transgene containing vector were subjected to cesium chloride isopycnic gradient. Fractions from the gradient were treated with DNase and RNase prior to dot blotting to remove unpackaged nucleic acids; fraction numbers are labeled above the dot blot. Fraction 1 has a density range of 1.377–1.41, fraction 2 has a density range of 1.39–1.435, and fraction 3 has a density range of 1.42–1.45. The β-galactosidease gene was used as the control template, to estimate particle numbers. Estimates of particle number where derived assuming 1 μg of 1000-bp DNA has 9.1×10^{11} molecules. (B) Infection of HeLa cells with 1.75×10^8 particles from various insertion mutants and wild-type capsid containing the LacZ transgene. Cells expressing the transgene appear blue when stained with X-gal.

purification technique is not as harsh as CsCl and has been shown to increase virus recovery by 10-fold (Zolotukhin *et al.,* 1999). However, other class II mutants remained noninfectious after purification using an iodixanol step gradient (data not shown). Although we determined that insertion mutant viruses N2944 and H3595 were infectious using the LacZ transduction assay, it should be noted that these mutants resulted in low infectious titers (1×10^2 transducing units/1.75×10^8 particles), similar to those of previously published low infectious particle (*lip*) mutants (Hermonat *et al.,* 1984).

Electron microscopy of class II and class III mutants

To further characterize class II and III rAAV2 insertion mutants for biological differences, we visualized mutant particles by EM. The EM analysis revealed only gross morphology of the infectious class III viruses, which were indistinguishable from wild-type virions (compare Figs. 4A with 4B and 4C). Whereas distinct differences were observed between class II/III mutant virus H3595 when compared to wild-type virions (Figs. 4A and 4F, bottom four panels). EM images of H3595 revealed a slightly larger roughly pentagonal outline, while wild-type virus appeared uniformed in size and was hexagonal. Interestingly, class II mutant H2634, which was negative for Vp1 or Vp2 by Western blot (Fig. 2, lane 2), appeared normal in morphology by EM analysis (Fig. 4D). Based on this analysis, virion morphology alone is not sufficient to distinguish class II mutants from class III since small insertions within the capsids can result in either nondetectable (Figs. 4B–4E) or noticeable alterations in virion structure (Fig. 4F, bottom four panels). However, this approach was able to provide additional data to our characterization of these linker insertion mutants (Fig. 4, compare A to F).

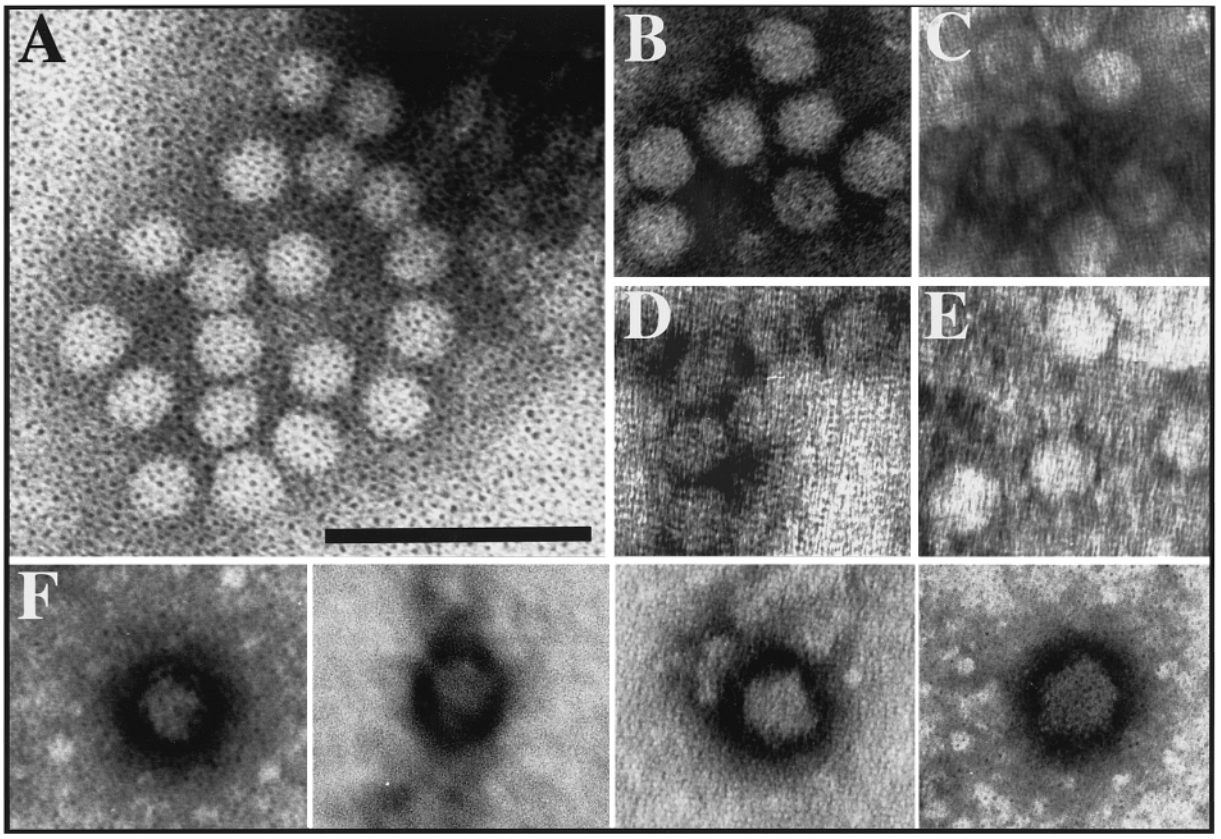

FIG. 4. Electron microscopy of insertion mutants. Samples (200 μl) of each virus from the peak fraction of gradient were dialyzed against 1× PBS + 1 mM $MgCl_2$, speed-vac desiccated, and then resuspended in 20 μl of distilled H_2O. Samples were negatively stained with 2% phosphotungstic acid. (A) rAAV2 with wild-type virion. Infectious insertion viruses (B) H2690 and (C) H2591. Noninfectious viruses (D) H2285, (E) H2634, and (F) H3595 (bottom four panels). The black bar in A is 100 nm; the magnification is equivalent in each panel.

Capsid ratio of class II and class III virions

Rose *et al.* (1971) established that AAV2 particles are composed of Vp1, Vp2, and Vp3 at a 1:1:20 ratio (Rose *et al.,* 1971). In an effort to determine if class II and class III mutant virions maintained this ratio, Western blots were performed on the cesium chloride-purified virus. Purified viruses analyzed by Western blot showed similar amounts of Vp3 in all mutants sampled (Fig. 5, Vp3 arrow); between 1×10^9 and 2.5×10^9 viral particles were used for each sample. The amounts of Vp2 and Vp1 are also nearly equivalent in all test samples, except H2634, where no minor capsid components were ob-

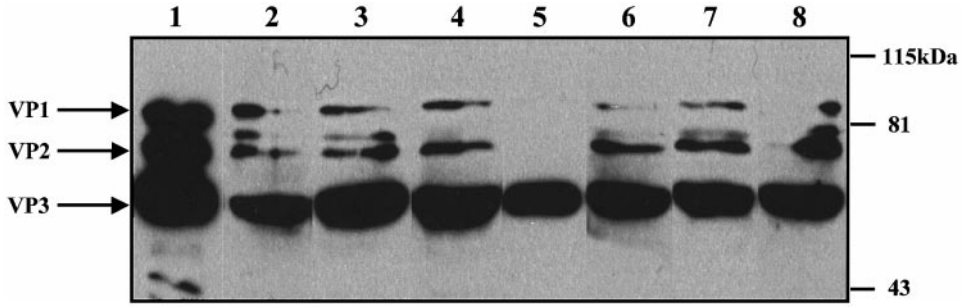

FIG. 5. Analysis of virion composition from wild-type and various insertion mutant viruses isolated from cell lysates by cesium chloride gradient centrifugation. Peak fractions of virus were determined by dot blot hybridization and dialyzed against 1× PBS + 1 mM $MgCl_2$. For each, viral sample between 1.0×10^9 and 2.5×10^9 particles were used. Virions from (1) wild-type rAAV2; (2) H2285; (3) R2349; (4) H2591; (5) H2634; (6) H2690; (7) H3766; and (8) N4160 were analyzed by acrylamide gel electrophoresis and immunoblotting with the B1 monoclonal antibody and detected by peroxidase-conjugated secondary antibody. On the right of the Western blot are the positions of the molecular weight standards and on the left are the positions of the major capsid protein, VP3, and the minor capsid proteins, VP2 and VP1.

served (Fig. 5, lane 5). The lack of minor capsid components for H2634 is consistent with the Western results from cell lysates (Fig. 2). At the limit of detection in this assay, the class II insertion mutant H2634 appears to assemble AAV virions without Vp1 and Vp2, even though EM analysis suggests that this mutant has normal morphology (Fig. 4D).

Heparin binding of class II and class III mutants

Recently our lab established that AAV-2 uses a heparan sulfate proteoglycan as a primary receptor for infectivity (Summerford and Samulski, 1998). To determine what role heparin binding may have in class II particles' inability to infect cells as well as the ability of class III virus to bind heparin agarose, heparin batch binding experiments were performed. Not surprisingly, all class III mutants were positive for heparin binding, with the majority of virus eluting in the 1 M $NaCl_2$ step (data not shown). To determine if loss of infectivity of class II mutant viruses was related to a lack of heparin binding, batch binding experiments were analyzed by dot blot hybridization (Fig. 6). For each of the viral samples tested, an internal control to determine 100% bound was spotted on the filter independently of heparin binding (Fig. 6, 100% bound). This allowed us to determine the percentage of virus retained, at each step of heparin purification. After binding to heparin agarose, samples were washed and then eluted using increasing salt concentrations (see Materials and Methods). Recombinant AAV2 with wild-type virion shells demonstrated 90% binding, with 10% released in the wash, followed by 60% recovered in the elution buffer, and 20% remaining bound to heparin agarose (Fig. 6, lane 1). Class II mutants H2285, H2416, and H2634 demonstrated similar binding and elution profiles (Fig. 6, lanes 2–4). However, class II mutant H3761 was distinct in its heparin agarose binding profile, with the majority of the virion in the binding buffer and the washes (Fig. 6, lane 5). Further analysis is required to determine the reason for lack of heparin binding in this batch assay.

Interestingly, H2634 binds heparin agarose under these conditions, which by Western blot does not carry detectable Vp1 or Vp2 subunits (Fig. 5, lane 4). The lack of Vp1 and Vp2 in H2634 and its ability to bind heparin agarose suggest that the heparin binding domain may be located in Vp3 capsid proteins.

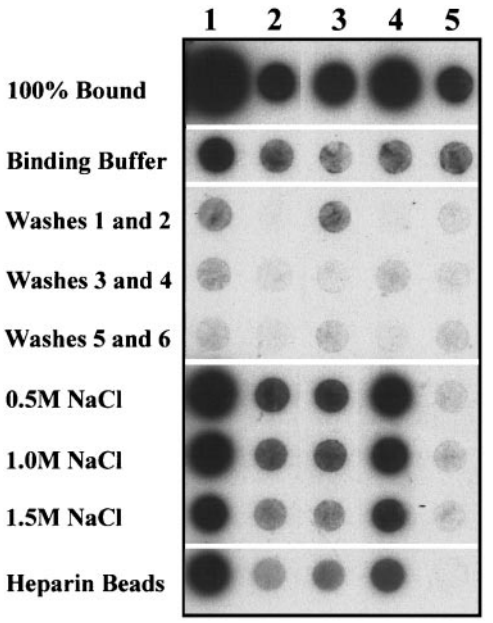

FIG. 6. Analysis of wild-type and noninfectious insertion mutant virus batch binding to heparin agarose by dot blot hybridization. Viruses with wild-type virions and insertion in the capsids were dialyzed against 0.5× PBS and 0.5 mM $MgCl_2$. One hundred microliters of each virus was bound to 100 μl of heparin agarose at room temperature for 1 h. Samples were washed six times with 500 μl of wash buffer each, followed by elution with 100 μl of 0.5, 1.0, and 1.5 M NaCl each, and the supernatant from each wash and elution step was saved. Twenty microliters of supernatant from each step and 20 μl of the agarose pellet were used for dot blot hybridization. Pairs of washes were combined and 1/50 of the total volume from each pair was used for dot blot hybridization, while 1/5 of the elution supernatant and agarose bed volumes was used. The 100% bound was equivalent to 1/5 of the virus added to the heparin agarose. Samples were (1) rAAV2 with wild-type virion; (2) H2285; (3) H2416; (4) H2634; and (5) H3761.

DISCUSSION

We have used insertional mutagenesis of the structural coding sequence of AAV serotype 2 in order to determine critical capsid domains and positions capable of tolerating insertions without loss of function. The linker insertions isolated were identified in each of the three AAV capsid subunits. Based on Western blot, cesium chloride isopycnic centrifugation, DNase protection, EM, as well as virus transduction analysis, we separated the capsid insertion mutants into three classes. The classes were distinguished based on whether the mutations resulted in inability to assemble virions (class I), ability to package and protect virion DNA (class II), and finally ability of assembled virions that protect viral DNA to infect target cells (class III).

To carry out this study, we used a cloning strategy that employed partial digestion of the capsid coding sequences to create a collection of in-frame linker insertion mutants. The restriction enzymes we utilized (*Hae*III *Nla*IV, and *Rsa*I) have 43 sites within this region of AAV2. Although this strategy appeared straightforward, of the enzymes chosen, only *Hae*III did not show a site preference. The restriction enzyme *Nla*IV showed a 25% site preference for position 4160, while *Rsa*I displayed a 45% site preference for position 3391. These site preferences hampered the inclusion of all 43 potential insertion sites in this study (Table 1). Regardless of these limitations, we were able to generate 22 insertion mutants that spanned all three capsid coding domains (Fig. 1). A critical aspect of this approach was the choice of the *Eco*RV restriction

site as part of the linker insertion. The sequence of this insert was chosen for two reasons: (1) *Eco*RV is not present in the AAV genome and (2) the 12-bp insertion would not produce a stop codon within any frame using these restriction enzymes. Incorporation of Kan^r gene between two *Eco*RV restriction sites allowed for easy isolation of plasmids carrying novel insertions (drug selection in *E. coli*). The Kan^r coding sequences was removed by *Eco*RV digestion and reforming a single 12-bp insertion site containing a unique *Eco*RV site within the capsid gene (Fig. 1). Following detailed mapping of linker insertion sites, the capsid coding sequences were subcloned into AAV helper plasmids previously established in our lab and assayed for AAV2 vector production. Utilizing the linker-modified helper plasmids, we were able to test rAAV vectors for virion assembly, capsid composition, stability, heparin binding, and infectivity.

Class I insertion mutants

Of the 22 capsid insertion mutants isolated, 7 were identified with a class I phenotype. Class I mutants did not protect the viral genome as assayed by DNase and dot blot hybridization of cesium chloride gradient fractions (data not shown). This class of capsid mutants may include both packaging and assembly defects. Additionally, some class I mutants may have reduced stability during purification through cesium chloride or temperature-dependent assembly. While we did not characterize these capsid variants further, these mutants are similar to *cap* mutants first described by Hermonat *et al.* (1984). The mutants described by Hermonat *et al.* (1984) were also defective for virus production (Hermonat *et al.,* 1984). Although defective for production of stable AAV virions, these mutants may be important reagents for studying AAV maturation.

For example, studies examining the subcellular location of wild-type AAV2 capsid subunits resulted in Vp3 dispersed throughout the cell, while Vp1 and Vp2 accumulate in the nucleus (Hunter and Samulski, 1992; Wistuba *et al.,* 1997). Using a conformation-specific antibody against assembled AAV2, nucleolar localization was shown (Wistuba *et al.,* 1997), similar to previous fluorescent antibody assays against AAV virions (Hunter and Samulski, 1992). Furthermore, when individual Vp1 and Vp2 capsid subunits were expressed in HeLa cells, wild-type patterns of distribution were observed. However, only when Vp3 was expressed in the presence of Vp1 or Vp2 did this protein also accumulate in the nucleus as previously described (Ruffing *et al.,* 1992). These results suggest that interactions between the subunits are important for the assembly of AAV2 particles even in the absence of terminal repeats or *rep* protein functions. Similar analysis of class I capsid subunit distribution may help demonstrate the presence of domains that are responsible for proper nuclear localization and assembly.

Class II insertion mutants

The class II insertion mutants isolated in this study protect the viral genome in a DNase assay, but are negative for virus infection. By Western blot analysis these mutants appear to assemble the virion with the same stoichiometry as wild-type virions (Fig. 2), with the exception of H2634. The linker insertions for this class were also distributed across all three capsid subunits (Table 1). The class II mutants described in this study appear distinct from the *cap* mutant category described previously (Hermonat *et al.,* 1984), in that although defective for infectious virions, these mutants accumulate and protect ssDNA. In addition, the majority of these mutants were positive for retention to a heparin column, suggesting that binding to the AAV primary receptor (heparan sulfate) was not a rate-limiting step (Summerford and Samulski, 1998). Surprisingly, one mutant, H2634, did not appear to express Vp1 and Vp2 in either cell lysates (Fig. 2) or purified virions (Fig. 5) but bound heparin sulfate similarly to the wild-type (Fig. 6). Although Vp1 and Vp2 could not be detected, EM analysis did not reveal any gross alteration in morphology (Fig. 4D). The absence of Vp1 and Vp2 is difficult to explain since it contradicts the requirement of these proteins to sequester Vp3 in the nucleus, as previously described (Hunter and Samulski, 1992; Ruffing *et al.,* 1992; Wistuba *et al.,* 1997). Although H2634 inserts an ADIG and the aspartic acid results in a net negative charge, the position of the ADIG is directly downstream of two lysines. The insertion of ADIG may cause a local misfolding of the capsid protein, exposing these or other lysines to ubiquitin-conjugating enzymes, thereby altering the half-life of Vp1 and Vp2 but not Vp3 (Hershko and Ciechanover, 1992). It is plausible that Vp1 and Vp2 are still able to sequester Vp3 to the nucleus for assembly but their shortened half-life reduces their incorporation in the assembled virion to levels undetectable by Western blots.

Since the class II mutants bound heparin, the loss of productive infection to HeLa and 293 cells appears unrelated to receptor binding. The viral entry pathway of AAV2 has not been extensively studied. Recent work has demonstrated that AAV2 enters the cell through an endosome and is released in a pH-dependent manor. This is followed by migration to the perinuclear space and uncoating in productive infections (Barlett, personal communication). A similar pathway is used by canine parvovirus, suggesting conservation in entry mechanism among these parvoviruses (Vihinen-Ranta *et al.,* 1998). The ability of class II mutants to bind heparin sulfate but fail to transduce target cells suggests a blocked in infection that may occur at any step from viral entry to

uncoating. Recently, we demonstrated the ability to assay early steps in AAV entry using fluorescent virus infused in rat brain (Bartlett and Samulski, 1998). These studies determined that the virus bound to target cells within 10 min, followed by transport to the nucleus within the first hour postinfection. Similar analysis using these mutants should be extremely helpful in better defining the defects of these mutants in early steps of AAV infection.

Class III insertion mutations

The class III mutants were unique in that they protected the viral genome and retained infectivity at levels near that of wild-type virus (Fig. 3B). Similar to class II, class III mutants protected viral DNA, bound heparin (data not shown), had normal morphologies by EM (Fig. 4B), and were derived from linker insertions positioned in each of the three capsid subunits (Table 1). The characterization of these capsid mutants represents the first description of AAV virions that can tolerate amino acid inserts without interfering with normal viral infectivity. In addition, these mutants validate the concept of expressing foreign epitopes on the surface of AAV capsids that may influence normal infectivity, such as retargeting. Previous modifications with B19 Vp1 and egg white lysozyme fusion proteins resulted in virus-like particles that retain lysozyme enzyme activity. While these data supported the ability to form capsid fusion proteins, the particles generated were empty and not infectious (Miyamura *et al.,* 1994). The viable class III mutants isolated in this study ranged from 5% (H2690) to 100% (N4160) of wild-type infectivity. Understanding the distinction between low infectious particles and high transducing particles should help determine critical steps in AAV infection. In addition, the wild-type viable insertion mutants provide a unique opportunity to test insert size limitation as well as ligand-specific retargeting of modified virions (Rabinowitz and Samulski, manuscript in preparation). Recently, the sequence and viral tropism of AAV serotypes 4 and 5 have been characterized (Chiorini *et al.,* 1999, 1997). These viruses do not appear to utilize heparan sulfate as a receptor for infection, and therefore domain swapping between serotypes should provide a unique opportunity to identify amino acids specific for viral binding to target cells (Rabinowitz and Samulski, manuscript in preparation). Detailed analysis of these mutants should provide a better understanding of both wild-type and vector-modified infection.

Two mutants (H/N2944 and H3595), which were first identified as class II after $CsCl_2$ gradient purification, demonstrated a class III phenotype when isolated using an iodixanol step gradient. Interestingly, mutants of this type have been described as *lip* (Hermonat *et al.,* 1984). However, unlike the *lip* mutants of Hermonat *et al.* (1984), which were positioned solely within the Vp1 unique coding region (Hermonat *et al.,* 1984), H/N2944 and H3595 were localized to Vp3. Interestingly, mutant H3595 displayed morphological differences by EM when compared to wild-type virions. This mutant had a pentagonal appearance and was slightly larger than the wild-type (Fig. 4D). Because the H3595 insertion is within a putative loop domain of Vp3 coding sequences, the alteration is present in all 60 subunits and results in the insertion of amino acids GRYRP (Table 1). A comparison of CPV and FPV crystal structures has determined that 5 of the 10 amino acid differences in Vp2 are on the surface of the virion (Llamas-Saiz *et al.,* 1996). One of these changes, 375 N-D, causes a displacement of 7 Å in the domain between loops 3 and 4 (Agbandje *et al.,* 1993). These examples demonstrate the significance of both genetic and crystal analysis when studying virion structure and function. The alteration seen with this virion by EM and *lip* phenotype observed after infection maybe due to the amino acid insertion interfering with capsid domain folding, number of assembled subunits, and or assembly symmetry. The exact explanation of this phenotype will require information obtained from AAV crystal structure analysis.

The availability of crystal structures for some of the parvoviruses has complemented genetic studies and provided sufficient detail to test critical domains involved in entry and infectivity. The parvovirus B19 crystal structure has been determined to 8 Å (Chapman and Rossmann, 1993). Although there is only a 15% overall identity between B19 and the feline panleukopenia virus (FPV) virion, the core antiparallel β-barrel of B19 is similar with respect to the overall symmetry of the antiparallel β-barrel in FPV (Agbandje-McKenna *et al.,* 1994). The eight antiparallel β-strands form a barrel domain that is well conserved not only among parvoviruses but also among many types of viruses (Chapman and Rossmann, 1993; Rossmann, 1989). The crystal structure of CPV has been determined at 2.8 Å (Tsao *et al.,* 1991). This information has allowed the precise positioning of amino acid residues with respect to the surface domains of the viral subunit. Amino acids 93 and 323 of CPV are required for maintenance of host range infectivity (Chang *et al.,* 1992), and from the crystal structure, these regions have been determined to be part of loops 1 and 3 (Tsao *et al.,* 1991). The crystal structure of FPV has been determined at 3.3 Å (Agbandje *et al.,* 1993).

In summary, we have generated a collection of AAV capsid mutants that fall into three phenotypes; class I mutants, which are defective for producing stable virions, class II mutants, which assemble noninfectious DNA intact virions, and class III mutant virions, which are infectious. We believe that these capsid mutants will be important reagents for analyzing basic questions of AAV infections that focus on virion assembly, receptor-mediated entry, uncoating, and viral transgene expression. The importance of understanding these fundamental

steps in AAV entry is best illustrated by recent studies using AAV vectors for cystic fibrosis gene therapy. These vectors have met with limited success due to the inability to infect target cells (Bartlett *et al.,* in preparation). The availability of these AAV class II and III capsid mutants will be valuable substrates for engineering rAAV vectors with novel targeting capabilities. In addition to deriving targeting vectors, further characterization of mutant capsids as well as the elucidation of the AAV crystal structure should provide a detail paradigm for AAV viral assembly and entry.

MATERIALS AND METHODS

Cells and viruses

Human 293 and HeLa cells were maintained at 37°C with 5% CO_2 saturation in 10% fetal bovine serum (Hyclone) in Dulbecco's modified Eagle's medium (Gibco BRL), with streptomycin and penicillin (Linberger Comprehensive Cancer Center, Chapel Hill, NC). Four $\times$ 10^6 293 cells were plated the day before transfection onto a 10-cm plate. Cells were transfected by both calcium phosphate (Gibco BRL) and Superfection (Qiagene) according to manufacturers' specifications. The insertional mutant packaging plasmids, described below, were transfected along with pAB11, containing the CMV-driven Lac Z gene with a nuclear localization signal. For each transfection the same amounts of packaging plasmid (12 μg) and pAB11 (8 μg) were used for each 10-cm plate. For each transfection an additional plate was used containing the transgene plasmid only to assess transformation efficiencies. After transfection the cells were infected with helper virus Ad5 *dl*309 at an M.O.I. of 5, and 48 h later the cells were lysed and the virus was purified.

Recombinant virus was purified using cesium chloride isopycnic or iodixanol gradients. In both cases cells were centrifuged at 1500 rpm (Sorvall RT 6000B) for 10 min at 4°C. Proteins were precipitated from the supernatant using ammonium sulfate (30% w/v) and resuspended in 1$\times$ phosphate-buffered saline (PBS) (137 mM NaCl, 2.7 mM KCl, 4.3 mM Na_2HPO_4 $7H_2O$, 1.4 mM KH_2PO_4). The cell pellet was resuspended in 1$\times$ PBS containing 0.1 mg/ml DNase I (Boehringer-Mannheim) lysed by three freeze–thaw cycles, combined with the protein portion of the supernatant, and incubated at 37°C for 30 min. This material was subjected to sonication (Branson Sonifier 250, VWR Scientific), 25 bursts at 50% duty, output control 2. Cell debris was removed by centrifugation (Sorvall RT 6000B). To each milliliter of supernatant 0.6 g of CsCl was added and the solution was centrifuged for 12–18 h (Beckman Optima TLX ultracentrifuge) in a TLS 55 rotor at 55,000 rpm. Alternatively, the supernatant was layered on top of an Iodixanol (OptiPrep-Nycomed Pharma As, Oslo, Norway) gradient of 60, 45, 30, and 15. This gradient was centrifuged in a Beckman Optima TLX ultracentrifuge using a TLN 100 rotor at 100,000 rpm for 1 h. Fractions were recovered from these gradients and 10 μl from each fraction was utilized for dot blot hybridization to determine which fraction contained the peak protected virion (see *Titration of recombinant virus*).

Construction of AAV packaging plasmids

The capsid domain of pAAV/Ad was cloned into pBS^+ (Stratagene) using *Hin*dIII, resulting in pAV2Cap. Partial digestion of pAV2Cap using the restriction enzymes *Hae*III, *Nla*IV, and *Rsa*I and gel purification of the unit-length DNA fragment resulted in the isolation of the starting material for cloning. The aminoglycoside 3′-phosphotransferase gene, conferring kanamycin resistance (Kan^r), from pUC4K (Pharmacia) digested with *Sal*I was flanked by linkers containing *Nae*I and *Eco*RV sites, a *Sal*I overhang at one end, and an *Eco*RI overhang at the other end (top 5′-AATTCGCCGGCGATATC-3′, bottom 5′-TCGAGATATCGCCGGC-3′). This fragment was cloned into the *Eco*RI site of pBluescript (SK^+) (Stratagene). Digestion with *Nae*I released the Kan^r gene, and this fragment was ligated into the pAV2Cap partials. The resulting plasmids were screened for insertion into the capsid domain and then digested with *Eco*RV to remove the kan^r gene, leaving the 12-bp insertion 5′-GGCGATATCGCC-3′ within the capsid domain. Multiple enzyme digests and DNA sequencing were used to determine the position of the 12-bp insertion within the capsid coding domain. The enzyme digests included *Eco*RV/*Ban*II, *Eco*RV/*Bst*NI, *Eco*RV/*Pst*I, and *Eco*RV/*Hin*dIII. The capsid domains of the resulting plasmids were digested with *Asp*718 and subcloned into the pACG2 packaging plasmid, with the exception of one *Nla*IV clone that overlapped the 3′-*Asp*718 site. This insertion mutant was cloned into pAAV/Ad using a *Hin*dIII/*Nsi*I digestion.

Western blotting

Cell lysates after freeze–thaw lysis and sonication was centrifuged to remove large cell debris. Twenty microliters of supernatant was immediately added to 20 μl of 2$\times$ SDS gel loading buffer containing dithiothreitol and boiled for 5 min. Proteins were analyzed by SDS–polyacrylamide gel electrophoresis and transferred to nitrocellulose electrophoretically. The nitrocellulose membranes were immunoblotted using the anti-Vp3 monoclonal antibody B1 (a generous gift from Jurgen A. Kleinschmidt). Each of the insertion mutants was tested at least twice by Western blot analysis. The secondary anti-mouse horseradish peroxidase IgG was used to indirectly visualize the protein by enhanced chemiluminescence (ECL, Amersham). The Western blots were scanned from enhanced chemiluminescence-exposed BioMax film (Kodak) into Adobe PhotoShop and analyzed by ImageQuaNT software (Molecular Dynamics Inc.).

Viral proteins were visualized by Western blotting fol-

lowed by immunoblotting as described above. Between 1.0 and 2.5 × 109 viral particles were used for each sample. The virus was isolated from the peak cesium gradient fraction as determined by dot blot and dialyzed against 0.5× PBS containing 0.5 mM $MgCl_2$ prior to polyacrylamide gel electrophoresis.

Titration of recombinant virus

Fractions from CsCl gradients were obtained by needle aspiration. The refractive index was obtained using a refractometer (Leica Mark II), and the index was used to determine the density of fractions. Aliquots of 10 μl from fractions between 1.36 and 1.45 g/ml were tested for the presence of protected particles by dot blot hybridization. The aliquots were diluted 1:40 in viral dilution buffer (50 mM Tris–HCl, 1 mM $MgCl_2$, 1 mM $CaCl_2$ 10 μg/ml RNase, 10 μg/ml DNase) and incubated at 37°C for 30 min. To the samples sarcosine (final concentration 0.5%) and EDTA (final 10 mM) were added and incubated at 70°C for 10 min. Proteinase K (Boehringer-Mannheim) was added to a final concentration of 1 mg/ml and the samples were incubated at 37°C for 2 h. Following this incubation the samples were denatured in NaOH (350 mM final) and EDTA (25 mM final). The samples were applied to equilibrated Nytran (Gene Screen Plus, NEN Life Science Products) using a dot blot manifold (Minifold I, Schleicher & Schuell). The membrane was probed with a random-primed (Boehringer-Mannheim) [^{32}P]dCTP-labeled LacZ DNA fragment. The membranes were exposed to film (BioMax MR, Kodak) or to phosphor imagining screens (Molecular Dynamics) and intensity estimates were done using ImageQuant software (Molecular Dynamics). Peak fraction of virus were then dialyzed in 1× PBS for transducing titer.

Transductions titers were determined by histochemical staining for LacZ activity. HeLa cells had been infected with Ad *dl*309 at a m.o.i. of 5 for 1 h. The cells were then washed with 1× PBS and fresh medium was added. Aliquots of virus from peak fractions, equivalent to 1.75 × 10^8 particles, were used to infect HeLa cells. Twenty to twenty-four hours later cells were washed with 1× PBS, fixed (2% formaldehyde, 0.2% gluteraldehyde in 1× PBS), washed, and stained with 5′-bromo-4-chloro-3-indoly-β-D-galactopyranoside (Gold Bio Technology) dissolved in *N,N*-dimethyl formamide (Sigma) diluted to 1 mg/ml in 1× PBS, pH 7.8, 5 mM potassium ferricyanide, 5 mM potassium ferrocyanide, 2 mM $MgCl_2$ at 37°C for 12–24 h. Stained HeLa cells were counted in ten 400× microscope fields. The transducing number was determined by averaging the number of stained cells in 10 fields, multiplying by the number of fields on the plate, and dividing that number by the number of nanograms of protected template.

Electron microscopy

Peak fractions of rAAV with wild-type virion or mutagenized virions were dialyzed in 0.5× PBS containing 0.5 mM $MgCl_2$. The virus was placed on a 400-mesh glow-discharged carbon grid by inverting on a 10-μl drop of virus for 10 min at room temperature, followed by three 1× PBS washes for 1 minute each. The virus was stained in 2% phosphotungstic acid for 1 min. Specimens were visualized using a Zeiss EM 910 electron microscope.

Heparin agarose binding assay

Recombinant virus containing wild-type capsids or insertion in the capsids were dialyzed against 0.5× PBS containing 0.5 mM $MgCl_2$. One hundred microliters of each virus was bound to 100 μl of heparin agarose type 1 (H-6508, Sigma, preequilibrated in 20 vol of 0.5× PBS containing 0.5 mM $MgCl_2$) at room temperature for 1 h in a 1.5-ml microfuge tube. After each step, binding washes and elutions samples were centrifuged at 2000 rpm (Sorvall MC 12V) for 2 min to collect supernatant. Samples were washed six times with 0.5 ml of 0.5× PBS containing 0.5 mM $MgCl_2$, and the supernatants collected. Samples were eluted in three steps of 100-μl volumes containing 0.5, 1.0, and 1.5 M NaCl in 0.5× PBS containing 0.5 mM $MgCl_2$ and the supernatants collected. For each sample 20 μl of supernatant from each step was used for dot blot hybridization. The 100% bound control was an internal standard equivalent to one fifth of each input virus used in the dot blot. The heparin agarose viral mixtures were washed six times with 0.5× PBS, 0.5 mM $MgCl_2$ in volumes that resulted in a 1:15,625 dilution.

ACKNOWLEDGMENTS

We acknowledge Shamasia Shafi, Mitch Sally, and Lisa Hanson for technical help and Terry Van Dyke for critical reading of the manuscript. Joseph Rabinowitz was supported by a grant from the Muscular Dystrophy Association. In addition, this work was supported by NIH Grants DK53423-01 and HL51818-06.

REFERENCES

Agbandje, M., McKenna, R., Rossmann, M., Strassheim, M., and Parrish, C. (1993). Structure determination of feline panleukopenia virus empty particles. *Proteins* **16,** 155–171.

Agbandje-McKenna, M., McKenna, R., Rossmann, M., Strassheim, M., and Parrish, C. (1994). The structure of human parvovirus B19 at 8 Å Resolution. *Virology* **203,** 106–115.

Atchison, R. W., Casto, B. C., and Hammond, W. M. (1965). Adenovirus-associated defective virus particles. *Science* **149,** 754–756.

Bartlett, J. S., and Samulski, R. J. (1998). Fluorescent viral vectors: a new technique for the pharmacological analysis of gene therapy. *Nature Med.* **4,** 635–637.

Becerra, S. P., Koczot, F., Fabisch, P., and Rose, J. A. (1988). Synthesis of adeno-associated virus structural proteins requires both alternative mRNA splicing and alternative initiations from a single transcript. *J. Virol.* **62,** 2745–2754.

Berns, K. I., and Adler, S. (1972). Separation of two types of adeno-

associated virus particles containing complementary polynucleotide chains. *J. Virol.* **5,** 693–699.

Berns, K. I., and Rose, J. A. (1970). Evidence for a single-stranded adeno-associated virus genome: Isolation and separation of complementary single strands. *J. Virol.* **5,** 693–699.

Brown, C., Welling-Wester, S., Feulbrief, M., Van Ient, J., and Spaan, W. (1994). Chimeric parvovirus B19 capsids for the presentation of foreign epitopes. *Virology* **198,** 477–488.

Casto, B. C., Atchison, R. W., and Hammon, W. M. (1967). Studies on the relationship between adeno-associated virus type I (AAV-I) and adenoviruses. I. Replication of AAV-I in certain cell cultures and its effect on helper adenoviruses. *Virology* **32,** 52–59.

Chang, S., Sgro, J., and Parrish, C. (1992). Multiple amino acids in the capsid structure of canine parvovirus coordinately determine the canine host range and specific antigenic and hemagglutination properties. *J. Virol.* **66,** 6858–6867.

Chapman, M., and Rossmann, M. (1993). Structure, sequence, and function correlations among parvoviruses. *Virology* **194,** 419–508.

Chiorini, J. A., Kim, F., Yang, L., and Kotin, R. M. (1999). Cloning and characterization of adeno-associated virus type 5. *J. Virol.* **73,** 1309–1319.

Chiorini, J. A., Yang, L., Liu, Y., Safer, B., and Kotin, R. M. (1997). Cloning of adeno-associated virus type 4 (AAV4) and generation of recombinant AAV4 particles. *J. Virol.* **71,** 6823–6833.

Hermonat, P. L., Labow, M. A., Wright, R., Berns, K. I., and Muzyczka, N. (1984). Genetics of adeno-associated virus: Isolation and preliminary characterization of adeno-associated virus type 2 mutants. *J. Virol.* **51,** 329–333.

Hershko, A., and Ciechanover, A. (1992). The ubiquitin system for protein degradation. *Annu. Rev. Biochem.* **61,** 761–807.

Hoggan, M. D., Blacklow, N. R., and Rowe, W. P. (1966). Studies of small DNA viruses found in various adenovirus preparations: Physical, biological, and immunological characteristics. *Proc. Natl. Acad. Sci. USA* **55,** 1457–1471.

Hunter, L. A., and Samulski, R. J. (1992). Colocalization of adeno-associated virus Rep and capsid proteins in the nuclei of infected cells. *J. Virol.* **66**(1), 317–324.

Janik, I. E., Huston, M. M., and Rose, J. A. (1984). Adeno-associated virus proteins: Origin of the capsid components. *J. Virol.* **52,** 591–597.

Li, J., Samulski, R. J., and Xiao, X. (1997). Role of highly regulated *rep* gene expression in adeno-associated virus vector production. *J. Virol.* **71,** 5236–5243.

Llamas-Saiz, A. L., Agbandje-McKenna, M., Parker, J. S. L., Wahid, A. T. M., Parrish, C. R., and Rossmann, M. G. (1996). Structural analysis of a mutation in canine parvovirus which controls antiginicity and host range. *Virology* **225,** 65–71.

McPherson, R. A., Rosenthal, L. J., and Rose, J. A. (1985). Human cytomegalovirus completely helps adeno-associated virus replication. *Virology* **147,** 217–222.

Miyamura, K., Kajigays, S., Momoeda, M., Smith-Gill, S., and Young, N. (1994). Parvovirus particles as platforms for protein presentation. *Proc. Natl. Acad. Sci. USA* **91,** 8507–8511.

Muralidhar, S., Becerra, S. P., and Rose, J. A. (1994). Site-directed mutagenesis of adeno-associated virus type 2 structural protein initiation codons: Effects on regulation of synthesis and biological activity. *J. Virol.* **68**(1), 170–176.

Myers, M. W., and Carter, B. J. (1981). Adeno-associated virus replication. *J. Biol. Chem.* **256,** 567–570.

Myers, M. W., Laughlin, C. A., Jay, F. T., and Carter, B. J. (1980). Adenovirus helper function for growth of adeno-associated virus: Effect of temperature-sensitive mutations in adenovirus early gene region 2. *J. Virol.* **35,** 65–75.

Rose, J. A., Berns, K. I., Hoggan, M. D., and Koczot, F. J. (1969). Evidence for a single-stranded adenovirus-associated virus genome: Formation of a DNA density hybrid on release of viral DNA. *Proc. Natl. Acad. Sci. USA* **64,** 863–869.

Rose, J. A., Maizel, J. K., and Shatkin, A. J. (1971). Structural proteins of adenovirus-associated viruses. *J. Virol.* **8,** 766–770.

Rossmann, M. G. (1989). The canyon hypothesis: Hiding the host cell receptor attachment site on a viral surface from immune surveillance. *J. Biol. Chem.* **264,** 14587–14590.

Ruffing, M., Heid, H., and Kleinschmidt, J. A. (1994). Mutations in the carboxy terminus of adeno-associated virus 2 capsid proteins affect viral infectivity: Lack of an RGD binding motif. *J. Gen. Virol.* **75,** 3385–3392.

Ruffing, M., Zentgraf, H., and Kleinschmidt, J. A. (1992). Assembly of viruslike particles by recombinant structural proteins of adeno-associated virus type 2 in insect cells. *J. Virol.* **66**(12), 6922–6930.

Samulski, R. J., Chang, L.-S., and Shenk, T. (1989). Helper-free stocks of recombinant adeno-associated viruses: Normal integration does not require viral gene expression. *J. Virol.* **63,** 3822–3828.

Sedlik, C., Saron, M., Sarraseca, J., Casal, I., and LecLerc, C. (1997). Recombinant parvovirus-like particles as an antigen carrier: A novel nonreplicative exogenous antigen to elicit protective antiviral cytotoxic T cells. *Proc. Natl. Acad. Sci. USA* **94,** 7503–7508.

Smuda, J. W., and Carter, B. J. (1991). Adeno-associated viruses having nonsense mutations in the capsid genes: Growth in mammalian cells containing an inducible amber suppressor. *Virology* **184,** 310–318.

Srivastava, A., Lusby, E. W., and Berns, K. I. (1983). Nucleotide sequence and organization of the adeno-associated virus 2 genome. *J. Virol.* **45,** 555–564.

Su, H., Raymond, L., Rockey, D. D., Fischer, E., and Hackstadt, T. (1996). A recombinant *Chlamydia trachomatis* major outer membrane protein binds to heparan sulfate receptors on epethelial cells. *Proc. Natl. Acad. Sci. USA* **93**(October), 11143–11148.

Summerford, C., and Samulski, R. J. (1998). Membrane-associated heparan sulfate proteoglycan is a receptor for adeno-associated virus type 2 virions. *J. Virol.* **72,** 1438–1445.

Tratschin, J.-D., Miller, I. L., and Carter, B. J. (1984). Genetic analysis of adeno-associated virus: Properties of deletion mutants constructed in vitro and evidence for an adeno-associated virus replication function. *J. Virol.* **51,** 611–619.

Trempe, J. P., and Carter, B. J. (1988). Alternate mRNA splicing is required for synthesis of adeno-associated virus VPI capsid protein. *J. Virol.* **62,** 3356–3363.

Tsao, J., Chapman, M. S., Agbandjo, M., Keller, W., Smith, K., Wu, H., Luo, M., Smith, T. J., Rossman, M. G., Compans, R. W., and Parrish, C. R. (1991). The three-dimensional structure of canine parvovirus and its functional implications. *Science* **25,** 1456–1464.

Vihinen-Ranta, M., Kalela, A., Makinen, P., Kakkola, L., Marjomaki, V., and Vuento, M. (1998). Intracellular route of canine parvovirus entry. *J. Virol.* **72,** 802–806.

Wistuba, A., Kern, A., Weger, S., Grimm, D., and Kleinschmidt, J. (1997). Subcellular compartmentalization of adeno-associated virus type 2 assembly. *J. Virol.* **71,** 1341–1352.

Zolotukhin, S., Byrne, B. J., Mason, E., Zolotukhin, I., Potter, M., Chesnut, K., Summerford, C., Samulski, R. J., and Muzyczka, N. (1999). Recombinant adeno-associated virus purification using novel methods improves infectious titer and yield. *Gene Ther.* **6,** 973–985.